# High Temperature Thermal Energy Storage Utilizing Metallic Phase Change Materials and Metallic Heat Transfer Fluids

**Johannes P. Kotzé**
e-mail: jpkotze@sun.ac.za

**Theodor W. von Backström**
e-mail: twvb@sun.ac.za

Department of Mechanical and Mechatronic Engineering,
Stellenbosch University,
Banghoek Road,
7600 Stellenbosch, South Africa

**Paul J. Erens**
Consulting Engineer

*Cost and volume savings are some of the advantages offered by the use of latent heat thermal energy storage (TES). Metallic phase change materials (PCMs) have high thermal conductivity, which relate to high charging and discharging rates in TES system, and can operate at temperatures exceeding 560 °C. In the study, a eutectic aluminium–silicon alloy, AlSi12, is identified as a good potential PCM. AlSi12 has a melting temperature of 577 °C, which is above the working temperature of regular heat transfer fluids (HTFs). The eutectic sodium–potassium alloy (NaK) is identified as an ideal HTF in a storage system that uses metallic PCMs. A concept is presented that integrates the TES-unit and steam generator into one unit. As NaK is highly reactive with water, the inherently high thermal conductivity of AlSi12 is utilized in order to create a safe concept. As a proof of concept, a steam power-generating cycle was considered that is especially suited for a TES using AlSi12 as PCM. The plant was designed to deliver 100 MW with 15 h of storage. Thermodynamic and heat transfer analysis showed that the concept is viable. The analysis indicated that the cost of the AlSi12 storage material is 14.7 US$per kWh of thermal energy storage.* [DOI: 10.1115/1.4023485]

*Keywords: PCM, AlSi12, NaK, CSP, eutectic, thermal energy storage*

## 1 Introduction

Solar thermal power generation could be feasible as a source of base load power in arid countries, but due to the intermittent and variable nature of the solar resource, an energy storage system is required. TES proves to be an attractive and economical alternative for large-scale use. Energy is accumulated in a storage medium, and the storage mechanism can be classified as sensible heat, latent heat, or chemical storage. Considering a review paper by Medrano et al. [1], it is clear that almost all operational solar thermal power stations use sensible heat thermal storage. The most popular sensible thermal storage systems use molten salts.

Currently, the cost of concentrating solar power (CSP) is the highest of all renewables [2]; therefore, cost reduction is the greatest priority of the CSP community. The use of higher efficiency power cycles is essential for cost reduction. Advanced high efficiency power cycles (like ultrasupercritical steam and supercritical $CO_2$) require thermal sources in the excess of 560 °C. This is above the temperature limits of the current state of the art thermal energy storage and HTFs.

Not only is the upper working temperature of current HTFs limited, but they solidify at temperatures above ambient. This is an issue that needs to be addressed by either using parasitic heating or a method of clearing the heat transfer pipes. This increases the operational and maintenance cost of the plant.

Latent heat storage materials or PCMs can store relatively large amounts of energy in small volumes, and thus have some of the lowest storage material costs per unit energy. Most PCMs operate between solid–liquid transitions, and are therefore most suitable as indirect storage concepts [3]. According to review papers [3,4], most of the potential salt-based PCMs have low thermal conductivity and extensive material or heat exchanger modifications need to be performed to yield feasible storage systems. This negates the cost savings through material reduction. Birchenall and Reichman [5] propose that eutectic metals may be used to store thermal energy in industrial processes; a concept that has been investigated by:

- He and Zhang [6], who developed a waste heat storage device using an eutectic alloy of silicon and aluminium (AlSi12);
- Wang et al. [7], who developed a space heater that stores thermal energy in AlSi12; and
- Sun et al. [8], who explored the use of AlMg34Zn6 as a storage material.

In this paper, a novel TES concept is proposed that is aimed at:

- allowing higher temperature heat transfer and thermal energy storage that will make the use of advanced power cycles feasible
- cost reduction of the storage unit by:
  (a) reducing the required volume of the necessary storage material
  (b) eliminating the need for material modification in the PCMs by using storage materials that inherently have high thermal diffusivity

## 2 Material Selection

The concept is subject to the thermophysical properties of the PCM and the HTF, and careful consideration is important. To illustrate the concept, a PCM and a HTF are identified and a concept for a TES unit and steam generator is proposed in Sec. 3.

**2.1 PCM.** Metallic PCMs offers the potential for high density, high temperature thermal energy storage [3]. They also have high thermal diffusivity which eliminates the need for large heat exchange surfaces. These factors may lead to significant reductions in levelized cost of electricity.

As noted by Kenisarin [4] in his review paper on investigated and proposed PCM materials, the two most important material properties of PCMs are the melting temperature and the heat of fusion of the material concerned. By plotting the melting temperature and heat of fusion of each material on a chart, it is possible to select a PCM with the most favorable characteristics for the design. As thermal high thermal diffusivity is a priority in the present case, only metallic PCMs are considered in the study. Figure 1 displays metallic PCMs plotted with melting temperature on the *x*-axis and heat of fusion on the *y*-axis.

Using Fig. 1, it is possible to identify a eutectic alloy of aluminium and silicon, AlSi12, as one of the best candidate metallic PCMs. It has a heat of fusion of 560 J/g and a melting point of 576 °C [7]. Li et al. [9] conducted a study on the suitability of aluminium–silicon alloys as PCMs. They found that aluminium–silicon alloys are relatively stable through multiple heating and cooling cycles, and that having an accurate eutectic composition and controlling cooling rates may improve stability.

Contributed by the Solar Energy Division of ASME for publication in the Journal of Solar Energy Engineering. Manuscript received January 26, 2012; final manuscript received January 7, 2013; published online May 14, 2013. Assoc. Editor: Rainer Tamme.

  

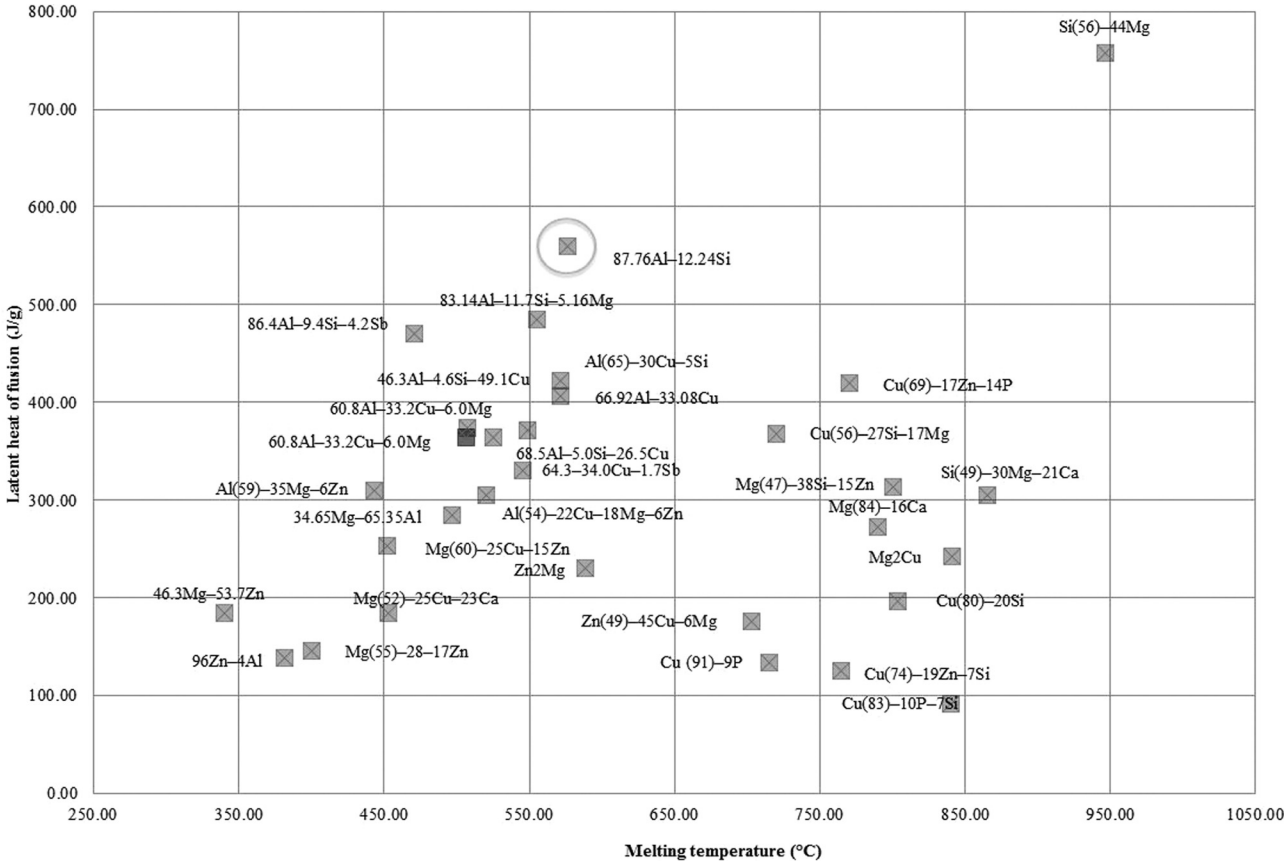


**Fig. 1 Latent heats and melting temperatures of metallic phase change materials [4; see Refs. 31 and 106] and [9]**

**2.2 HTFs.** To use AlSi12 (or any other alloy) as a PCM, an appropriate HTF is needed for the primary heat transfer loop of the power-generating cycle. The HTF should have the following properties:

- melting point below the night time temperature of a typical CSP-site
- reasonable specific heat capacity
- and low vapor pressure

Metallic heat transfer fluids in general have good high temperature heat transfer properties, but NaK was identified as an ideal candidate HTF for CSP. NaK is a eutectic alloy of sodium and potassium, and has the following properties [10]:

- composition: 22% Na, 78% K (by mass)
- melting point: −12.8 °C
- boiling point$_{@101\ kPa}$: 785 °C
- density: 724 kg/m$^3$
- specific heat capacity: 0.879 kJ/kg K
- viscosity: 0.000176 Pa s
- safety: Reacts violently with water

Although NaK is very reactive with water, the concept has been developed in a way to ensure that water and NaK will not be in close proximity to each other.

## 3 Concept

The high reactivity of NaK is a concern in the CSP industry. For this reason a concept is proposed that physically separates the NaK from the steam or water. This is achievable by utilizing the inherently high thermal conductivity of metal alloys. The idea is that the AlSi12 thermally buffers the primary NaK loop from the steam/water heat transfer pipes. The AlSi12 acts as a thermal capacitor. Figure 2 portrays a scaled-down cross-section of the storage container to illustrate the concept.

The NaK is pumped through the primary heat transfer loop (see Fig. 3) where the solar receiver heats it up. The NaK is then pumped through stainless steel heat transfer bundles in the thermal storage tanks where thermal energy is transferred to the AlSi12 at 577 °C. The AlSi12 is at its melting temperature, and the heat transferred to it from the NaK increases the saturation of the melt. The steam and water pipes also run through the storage tanks and cool down the AlSi12-melt. The superheated steam that is generated by cooling the AlSi12 is then used to drive turbines.

The storage tank is divided into three separate sections, each serving as a distinct part of the steam generator. The reason for this is that the heat transfer mechanisms of these parts are distinctly different.

In practical implementations of this concept, the melting point of the PCM will have to be adapted to better match temperature of the steam. In this analysis, all the sections will use AlSi12 as a PCM and the heat exchangers are divided up as follows:

(1) boiler
(2) superheater
(3) reheater

This configuration is dependent on the specific power-generating cycle used, shown in Fig. 3.

## 4 Thermodynamic Cycle

It is necessary to base the thermodynamic and heat transfer analysis on representative system boundary values in order to develop a proof of concept. Therefore, a hypothetical generating cycle had to be designed that would be representative of what

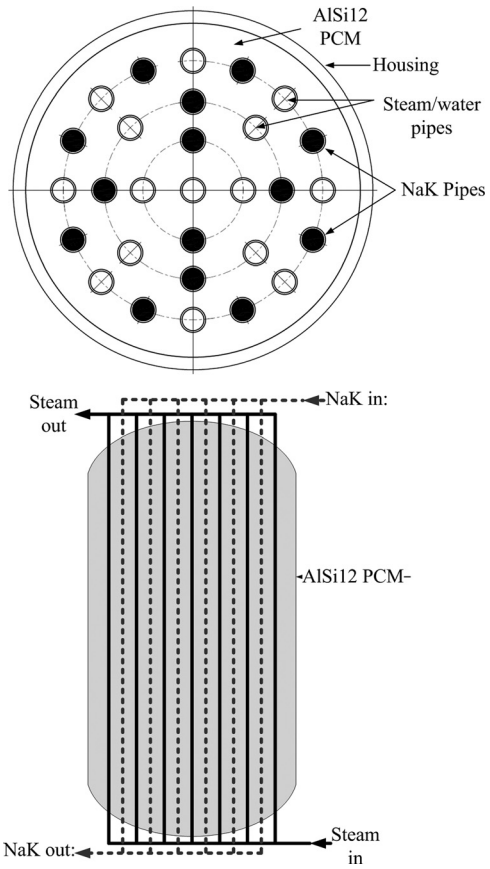


**Fig. 2 Cross-section of the storage container showing NaK and steam heat transfer pipes**

would typically be used for such a concept. The analysis is based on the following power cycle (depicted in Fig. 3):

- 100 MW electrical output;
- live steam conditions:
  (a) 540 °C superheat
  (b) 150 bars;
- reheat conditions:
  (c) 540 °C superheat
  (d) 30 bars
- open feed water heater with steam bled from the high pressure (HP) turbine exhaust
- low pressure (LP) turbine; and
- air-cooled condenser (ACC) with a condenser pressure of 0.15 bar

**Table 1 Steam cycle boundary values**

| | Inlet enthalpy (kJ/kg) | Outlet enthalpy (kJ/kg) | Mass flow rate (kg/s) | $\dot{Q}$(MW) |
|---|---|---|---|---|
| Boiler | 1026 | 2624 | 86 | 131 |
| Superheater | 2624 | 3457 | 86 | 69 |
| Reheater | 3546 | 2477 | 69 | 36 |
| Total | | | | 236 |

The power cycle presented in Fig. 3 was simulated in Flownex SE. Flownex is a network based analytical tool for the design and analysis of thermodynamic, heat transfer, and flow problems. The system was designed and analyzed in both transient and steady state conditions. The boundary conditions of the subsections (boiler, superheater, and reheater) of the steam generator were obtained. Table 1 presents the constant thermal power output of the three heat transfer sections in the steam generator under nominal conditions. This is used to size the storage system and the heat transfer surfaces.

## 5 Heat Transfer Calculations and Storage System Design

For heat transfer calculations and system sizing, the following thermophysical properties were used:

- melting point of AlSi12: 576 °C [7]
- heat of fusion of $AlSi12_{@577}$: 560 kJ/kg [7]
- density of $AlSi12_{@577}$: 2700 kg/m$^3$ [7]
- thermal conductivity of the following:
  (a) $AlSi12_{@577\,°C}$ 160 W/m K [7]
  (b) $steel_{@577\,°C}$ 39.2 W/m K

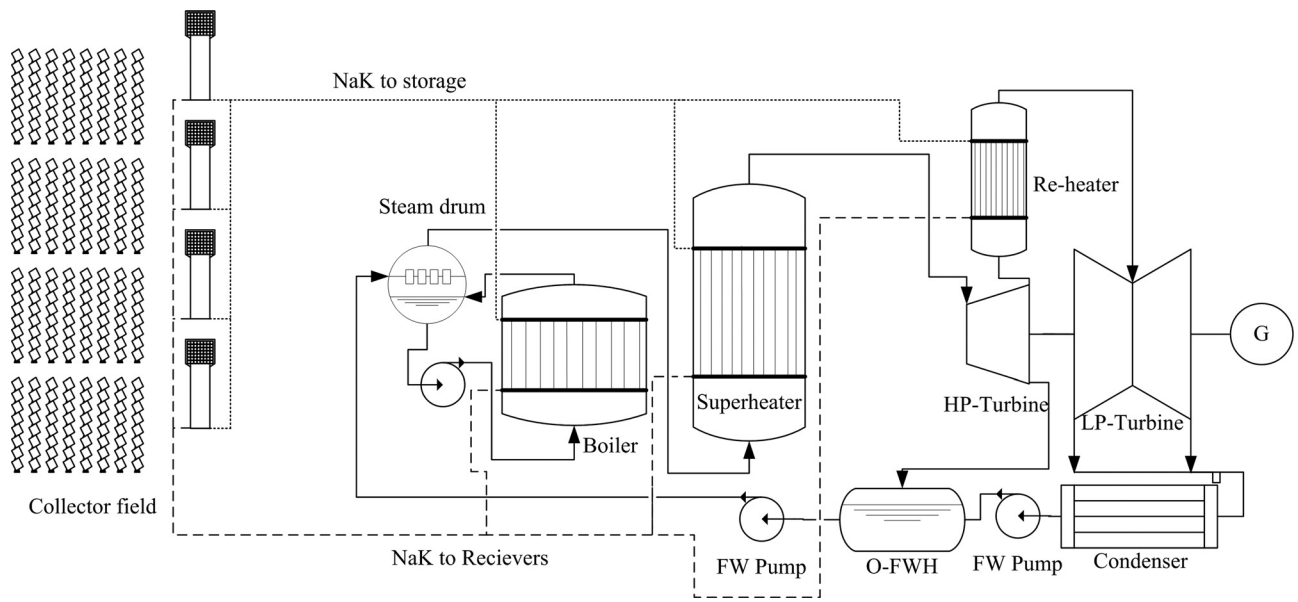


**Fig. 3 Power-generating cycle**

**Table 2 Required storage material**

| | $\dot{Q}$(MW) | Stored energy (GJ) | Mass (metric ton) | Volume ($m^3$) |
|---|---|---|---|---|
| Boiler | 131 | 7101 | 12,680 | 4785 |
| Superheater | 69 | 3634 | 6478 | 2445 |
| Reheater | 36 | 1453 | 2585 | 975 |
| Total | 236 | 12,188 | 21,743 | 8205 |

**Table 3 Tank configuration**

| | | Boiler | Superheater | Reheater |
|---|---|---|---|---|
| Number of tanks | | 10 | 8 | 4 |
| Diameter of individual tanks | (m) | 11 | 7 | 11 |
| Height of individual tanks | (m) | 6 | 5 | 5 |

(c) stainless steel$_{@577\,^\circ C}$ 20.8 W/m K

- specific heat of AlSi12$_{@577\,^\circ C\ (molten)}$: 1.038 kJ/kg K [7]
- steam and water: IAPWSIF97 standard throughout
- NaK: sodium-NaK engineering handbook

All calculations mentioned in Secs. 5.1 through 6 are based on these values.

**5.1 Storage System Sizing.** For the system to deliver base load power, it should operate at full power (100 MWe) for 24 h per day. The number of hours of energy storage needed is site-dependent but as this is a hypothetical plant, 15 h of storage was selected. By using the boundary values presented in Table 1, it is possible to determine the mass and volume of storage material needed. The results are shown in Table 2.

The PCM is stored in tanks. The geometries of the tanks are presented in Table 3. The storage tanks are divided up to reduce the size of the individual containment tanks, and to vary the heat exchanger geometry according to requirements.

**5.2 Water Side Heat Transfer and Heat Exchanger Design.** The basic variables of the heat exchangers in the steam generator sections include the length of the heat transfer pipes; the number of tubes; and the tube size. A discretized model of these heat transfer surfaces is implemented in Flownex; and the model is then used to obtain the sizing of the heat transfer surfaces using an optimization routine.

The Flownex heat transfer model can be best described through a resistance diagram as the heat transfer model is based on nodes. Material and fluid properties are evaluated using an extensive properties database.

In the model, it is assumed that the AlSi12 will solidify concentrically around the heat transfer pipes. And therefore will form concentric cylinders of solid AlSi12, which will have to be accounted for.

Figure 4 below shows a section through one of the heat transfer pipes, the thermal resistance network diagram is depicted below it. This model is generic for all three steam generator sections.

The convective boiling or convective resistances depend on which part of the steam generator is analyzed. In the reheater and superheater, the heat transfer mechanism is purely convective; in which case the Gnielinski [11] equation is used to calculate the Nusselt number.

In the boiler, the heat transfer mechanism is convective or flow boiling and is a two-phase flow problem. The homogeneous model is used for the calculation of the two-phase flow. The onset of nucleate boiling saturated boiling and Leidenfrost points are calculated automatically in Flownex. The heat transfer coefficient is calculated using the Steiner and Taborek [12] correlation. In transition boiling, a linear extrapolation between the critical heat flux

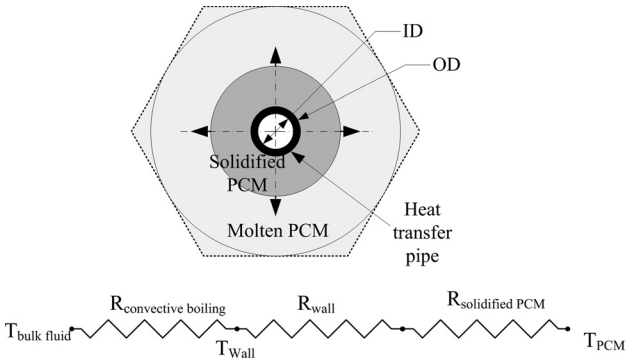


**Fig. 4 Section through one stem pipe showing annotation for analysis**

**Table 4 Steam/water heat exchange surfaces**

| | | Boiler | Superheater | Reheater |
|---|---|---|---|---|
| Number of steam pipes | | 300 | 410 | 500 |
| Diameter of steam pipes | (mm) | 33.4 | 33.4 | 33.4 |
| Wall thickness | (mm) | 4.55 | 4.55 | 4.55 |
| Length | (m) | 6 | 10 | 10 |
| Material | | MS | MS | MS |

and the minimum heat flux points is used [11]; and for film boiling the Zuber correlation is used [11].

On the PCM side of the heat transfer surfaces (the heat transfer pipes are embedded in the PCM), there is a moving boundary problem. As the storage system discharges, solidified PCM builds up around the heat transfer pipes, causing a variation in the heat transfer characteristics of the heat exchange surfaces.

The diameter of this PCM build-up is modeled in the storage model and is used in the heat transfer model. For the plant to operate at steady conditions, the effect of the moving boundary needs to be recognized. There is nothing that can be explicitly controlled about the energy source to the heat transfer surfaces (as in a gas-fired boiler), and the only feasible method of control is to manage the flow in the heat exchangers.

Flow boiling is a function of both convective-boiling heat transfer and nucleate boiling heat transfer [13]. Thus, to have a controllable steam generator, the convective or convective-boiling heat transfer should be the controlling heat transfer mechanism in the heat exchanger, especially close to complete discharge. All the steam generator sections have been designed so that the flow rate in the heat exchangers can be varied to control the heat transfer to the steam.

The geometry of the steam and water heat exchange surfaces are summarized in Table 4.

**5.3 NaK Side Heat Transfer and Heat Exchanger Design.** The isothermal nature of the storage unit decouples the heat transfer of the steam heat exchangers from that of the NaK heat exchangers; allowing the NaK loop to be considered separately. The modeled thermal input is based on the Bird clear sky model [14] for a winter's day in Upington.

The time-dependent thermal input of the model is based on the normalized direct normal irradiation (DNI) output of the Bird clear sky model. This is shown in Fig. 5, where the normalized DNI for both winter and summer are depicted by solid lines. As the hypothetical plant is required to operate at base load throughout the year, the system will be designed to cope with a winter scenario.

The required thermal energy to be collected and transferred into the storage system is equal to the product of the constant thermal output of the steam generator and 24 h. By integrating the normalized DNI, it is possible to determine how much the normalized DNI needs to be scaled to yield a solar input profile that will

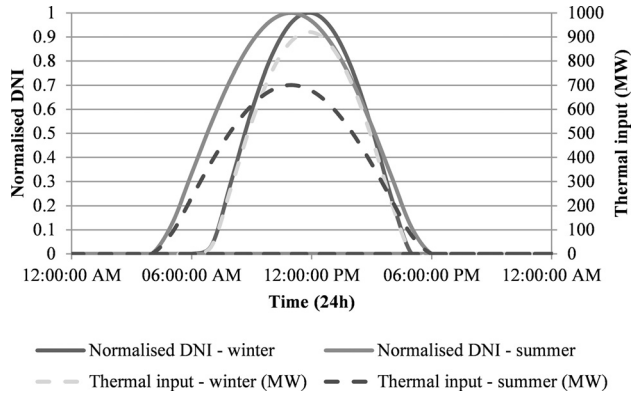


**Fig. 5 Normalized DNI and thermal input profiles for Upington for summer and winter**

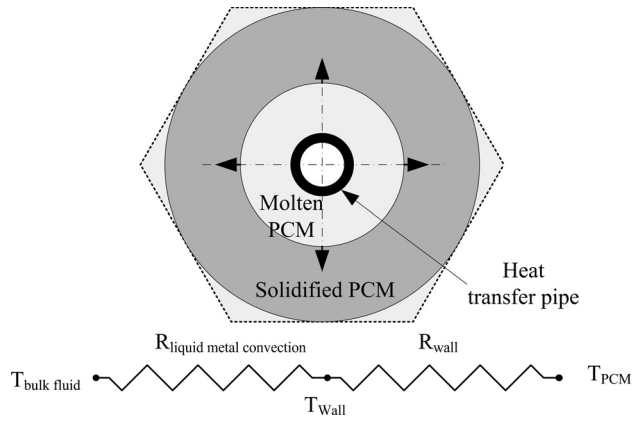


**Fig. 6 NaK heat transfer model**

deliver enough thermal energy to the storage units to operate the entire plant.

Using the winter thermal input profile, it is also possible to determine the peak heat transfer conditions that are required from the primary cooling loop. The heat transfer requirements for solar noon on a winter's day are presented in Table 6. The receiver temperature is a function of the mass flow rate of the NaK through the receiver. The receiver temperature will have to be determined through an economical optimization and is outside the scope of this paper.

A heat transfer model is needed for the sizing of the heat transfer surfaces of both the receiver and the heat exchangers in the storage units. The fluid properties of eutectic NaK is used, as specified in the *Liquid Metals Engineering Handbook* [10].

The heat transfer model that describes the NaK-AlSi12 heat transfer system is depicted in Fig. 6. Instead of solidified PCM accumulating around the heat transfer pipes, the AlSi12 melts around the heat transfer pipe, and the radius of molten PCM will continue to increase.

The Nusselt number for the liquid metal convective heat transfer is calculated using the Seban–Shimazaki correlation [10]. This heat transfer model has been implemented in Flownex and the accuracy of the model has been improved by further discretization of the heat transfer elements.

The design geometry was calculated using the conditions in Table 6 as the maximum heat transfer requirements through the day. The Flownex model yielded the design geometry summarized in Table 5. The inlet and outlet conditions of the heat exchangers are presented in Table 6.

## 6 Cost and Concept Advantages

The cost of the storage material is an important consideration. As the mass of storage material and amount of energy that needs to be stored are known from Table 2, the normalized cost of the storage material can be calculated in US$/kWh. AlSi12 cost 2 270 US$per metric ton [15]. The mass of storage material is 21 743 metric ton and the energy to be stored is 12 188 GJ (or 3 388 202 kWh). The normalized cost of the storage material is therefore calculated as 14.6 US$/kWh. Compared to salts that have material costs between five and 20 US$/kWh [16], this figure is competitive. It would, however, be a misrepresentation to make a comprehensive cost comparison based on this value. It is accordingly submitted that a detailed study on the entire plant is necessary for an accurate cost evaluation.

Higher temperature heat transfer and thermal energy storage also makes it possible to utilize higher efficiency thermodynamic cycles (like supercritical $CO_2$ and ultrasupercritical water cycles). This will further reduce storage cost and significantly decrease the number of heliostats needed.

Another advantage that NaK has is that there is no risk that the HTF can solidify at night. The concept may be improved by heating the storage material into the sensible region; thereby, increasing its storage capacity. Further improvements are possible by using multiple PCMs and various melting temperatures in a cascading fashion to reduce entropy generation in the boiler and preheater, and reducing the NaK flow rates.

**Table 5 NaK heat transfer surfaces**

| | | Boiler | Superheater | Reheater |
|---|---|---|---|---|
| Number of steam pipes | | 3730 | 2360 | 1225 |
| Diameter of steam pipes | (mm) | 21.24 | 21.24 | 21.24 |
| Wall thickness | (mm) | 2.77 | 2.77 | 2.77 |
| Length | (m) | 6 | 5 | 5 |
| Material | | SS | SS | SS |

**Table 6 NaK heat transfer conditions at peak solar noon in winter**

| | | Boiler | Superheater | Reheater | Receiver |
|---|---|---|---|---|---|
| NaK flow rate | (kg/s) | 5554 | 2923 | 1510 | 10,000 |
| Heat transfer requirements | (MW) | 511 | 269 | 139 | 920 |
| Inlet temperature | (°C) | 690 | 690 | 690 | 589 |
| Outlet temperature | (°C) | 560 | 589 | 589 | 690 |

## 7 Conclusion

The use of a metallic PCM offers a number of prospective advantages such as enabling the use of high efficiency power cycles, material cost savings, and high charging and discharging rates with minimal material modification. By making use of a comparative study, it was found that AlSi12 is an effective candidate material for a TES-concept. The sodium–potassium alloy, NaK, was identified as an ideal HTF for use in thermal storage. NaK does, however, yield an inherent safety risk in a steam cycle due to its reactivity to water. A concept was developed that utilizes the high thermal conductivity of AlSi12 to deliver a safe design for a combined TES-unit and a steam generator. Thermodynamic and heat transfer analysis proved that such a design is feasible, and the cost of the storage material provisionally appears to be competitive with that of solar salts.

The full financial benefit that this concept offers above that of salt storage is still unclear as there are a number of factors to be considered (technical and economic). Further research in this regard is therefore recommended, particularly if one considers the prospective advantages of this concept. A time-dependant analysis of the concept may furthermore shed important light on the economic feasibility of the concept. The use of different metal alloys

in a similar concept may also yield a more optimal overall system by reducing entropy generation. Further research in this regards is still on-going.

## Acknowledgment

The authors would like to thank the Centre for Renewable and Sustainable Energy Studies. The financial assistance of the National Research Foundation (NRF) toward this research is hereby acknowledged. (Opinions expressed and conclusions arrived at, are those of the author and are not necessarily to be attributed to the NRF). The Department of Science and Technology of South Africa through the Solar Thermal Spoke fund and the Stellenbosch University Hope project. Flownex SE for their generous license agreement.

## Nomenclature

AlMg32Zn6 = an aluminium alloy with 32% magnesium and 6% Zink by weight
AlSi12 = an aluminium alloy containing 12% silicon by weight
CSP = concentrating solar power
HTF = heat transfer fluid
NaK = a eutectic alloy of sodium and potassium
PCM = phase change material
TES = thermal energy storage

## References

[1] Medrano, M., Gil, A., Martorell, I., Potau, X., and Cabeza, L. F., 2010, "State of the Art on High-Temperature Thermal Energy Storage for Power Generation: Part 2—Case Studies," Renewable Sustainable Energy Rev., **14**, pp. 56–72.
[2] International Energy Agency, 2010, Technology Roadmap: Concentrating Solar Power, available at: http://www.iea.org/publications/freepublications/publication/csp_roadmap.pdf
[3] Gil, A., Medrano, M., Martorell, I., Lazaro, A., Dolado, P., Zalba, B., and Cabeza, L. F., 2010, "State of the Art on High Temperature Thermal Energy Storage for Power Generation: Part 1—Concepts, Materials and Modellization," Renewable Sustainable Energy Rev., **14**, pp. 31–55.
[4] Kenisarin, M. M., 2010, "High-Temperature Phase Change Materials for Thermal Energy Storage," Renewable Sustainable Energy Rev., **14**, pp. 955–970.
[5] Birchenall, C. E., and Reichman, A. F., 1979, "Heat Storage in Eutectic Alloys," Metall. Trans. A, **11A**, pp. 1415–1420.
[6] He, Q., and Zhang, W., 2001, "A Study on Latent Heat Storage Exchangers With the High-Temperature Phase-Change Material," Int. J. Energy Res., **25**, pp. 331–341.
[7] Wang, X., Liu, J., Zhang, Y., Di, H., and Jiang, Y., 2006, "Experimental Research on a Kind of Novel High Temperature Phase Change Storage Heater," Energy Convers. Manage., **47**, 2211–2222.
[8] Sun, J. Q., Zhang, R. Y., Liu, Z. P., and Lu, G. H., 2007, "Thermal Reliability Test of Al-34%Mg-6%Zn Alloy as Latent Heat Storage Material and Corrosion of Metal With Respect to Thermal Cycling," Energy Convers. Manage., **48**, pp. 619–624.
[9] Li, F., Hu, Y., and Zhang, R., 2011, "The Influence of Heating-Cooling Cycles on the Thermal Storage Performances of Al-17 Wt.% Si Alloy," Adv. Mater. Res., **239–242**, pp. 2248–2251.
[10] U.S. Atomic Energy Commission, 1974, "Liquid Metal Fast Breeder Reactor Program: Environmental Statement," Vol. 4, University of California Libraries, Oakland, CA.
[11] Flownex Simulation Environment, 2011, Flownex Theory Manual, www.flownex.com
[12] Steiner, D., and Taborek, J., 1992, "Flow Boiling Heat Transfer in Vertical Tubes Correlated by an Asymptotic Model," Heat Transfer Eng., **13**, pp. 43–69.
[13] Chen, J. C., 1966, "A Correlation for Boiling Heat Transfer to Saturated Fluids in Convective Flow," Ind. Eng. Chem. Process Des. Dev., **5**, pp. 322–329.
[14] Bird, R. E., and Hulstrom, R. L., 1991, "A Simplified Clear Sky Model for Direct and Diffuse Insolation on Horizontal Surfaces," SERI Technical Report SERI/TR-642-761, pp. 642–761.
[15] Mineral Fund Advisory, accessed July 13, 2011, www.mineralprices.com
[16] Herrmann, U., 2001, "Engineering Evaluation of a Molten Salt HTF in a Parabolic Trough Solar Field," accessed July 13, 2011, www.nrel.gov/csp/troughnet/pdfs/ulf_herrmann_salt.pdf